THE JOURNAL OF BIOLOGICAL CHEMISTRY
Vol. 279, No. 41, Issue of October 8, pp. 42954–42963, 2004
Printed in U.S.A.

Targeting, Import, and Dimerization of a Mammalian Mitochondrial ATP Binding Cassette (ABC) Transporter, ABCB10 (ABC-me)*

Received for publication, May 6, 2004, and in revised form, June 16, 2004
Published, JBC Papers in Press, June 23, 2004, DOI 10.1074/jbc.M405040200

Solomon A. Graf‡§¶‖, Sarah E. Haigh‡§¶, Erica D. Corson‡§, and Orian S. Shirihai‡§**

From the ‡BioCurrents Research Center, Marine Biological Laboratory, Woods Hole, Massachusetts 02543 and §Department of Pharmacology, Tufts University, Boston, Massachusetts 02111

ATP binding cassette (ABC) transporters are a diverse superfamily of energy-dependent membrane translocases. Although responsible for the majority of transmembrane transport in bacteria, they are relatively uncommon in eukaryotic mitochondria. Organellar trafficking and import, in addition to quaternary structure assembly, of mitochondrial ABC transporters is poorly understood and may offer explanations for the paucity of their diversity. Here we examine these processes in ABCB10 (ABC-me), a mitochondrial inner membrane erythroid transporter involved in heme biosynthesis. We report that ABCB10 possesses an unusually long 105-amino acid mitochondrial targeting presequence (mTP). The central subdomain of the mTP (amino acids (aa) 36–70) is sufficient for mitochondrial import of enhanced green fluorescent protein. The N-terminal subdomain (aa 1–35) of the mTP, although not necessary for the trafficking of ABCB10 to mitochondria, participates in the proper import of the molecule into the inner membrane. We performed a series of amino acid mutations aimed at changing specific properties of the mTP. The mTP requires neither arginine residues nor predictable α-helices for efficient mitochondrial targeting. Disruption of its hydrophobic character by the mutation L46Q/I47Q, however, greatly diminishes its efficacy. This mutation can be rescued by cryptic downstream (aa 106–715) mitochondrial targeting signals, highlighting the redundancy of this protein's targeting qualities. Mass spectrometry analysis of chemically cross-linked, immunoprecipitated ABCB10 indicates that ABCB10 embedded in the mitochondrial inner membrane homodimerizes and homo-oligomerizes. A deletion mutant of ABCB10 that lacks its mTP efficiently targets to the endoplasmic reticulum. Quaternary structure assembly of ABCB10 in the ER appears to be similar to that in the mitochondria.

ABC[1] transporters comprise a large and diverse family of membrane translocases (1). Their function ranges from peptide transport to phospholipid flipping to anion channel formation. Members of the ABC transporter superfamily have been implicated in numerous human diseases (including cystic fibrosis (CFTR/ABCC7), adrenoleukodystrophy (ALDP/ABCD1), Zellweger's syndrome (PMP70/ABCD3), progressive familial intrahepatic cholestasis (SPGP/ABCB11), and Stargardt macular dystrophy (ABCR/ABCA4)) (2). The basic structure of ABC transporters is relatively well conserved and includes a hydrophilic ATP binding cassette and a hydrophobic membrane-spanning domain (3). Whereas the large members of the family contain two of each domain, the "half-transporters" contain one of each and are predicted to dimerize (3–6). Mammalian ABC transporters are found predominantly in the plasma membrane but are also known to play essential roles in a number of organelles, including the endoplasmic reticulum, peroxisome, and the mitochondrion (2). Mammalian mitochondrial ABC transporters have recently gained attention for their role in heme biosynthesis and iron sulfur cluster synthesis (7–12). Accordingly, their involvement in the pathophysiology of acquired and inherited forms of sideroblastic anemias has been suggested and, in the case of ABCB7, already demonstrated. Only eight mitochondrial ABC transporters have been described to date (7). This is remarkable, given that in bacteria, ABC proteins are the most diverse family of transporters, numbering well over 50 in *Escherichia coli*. Since mitochondrial ABC transporters are synthesized in the cytosol, they require proper trafficking, import, and assembly to achieve functionality in their target organelle.

Two dominant mitochondrial import pathways have been described, each involving specialized import machinery and distinct signals (13). One pathway recognizes a cleavable, N-terminal mitochondrial targeting presequence (mTP) and is generally utilized by hydrophilic proteins. The second pathway, employed by the membrane metabolite carrier class of proteins, is used by more hydrophobic proteins bearing internal targeting signals. mTPs, although they lack a consensus primary sequence, share a number of common characteristics. They are rich in arginine residues, feature a net positive charge, and possess amphiphilic α-helices (14–17). Additionally, some mTPs include a short hydrophobic motif that is recognized by Tom20, a component of the mitochondrial import machinery on the outer membrane (18, 19). mTPs lead their preproteins into the matrix in a linear configuration, where they are cleaved off by the mitochondrial processing peptidase, allowing for final assembly of the mature protein in one of the mitochondrion's compartments (20). Proteins of the metabolite carrier class do not possess a cleavable presequence (21, 22). Rather, they bear three internal targeting modules that cooperatively bind to Tom70. These proteins are transported in a loop configuration directly into the inner membrane, where they assume their functional structure (23).

ABC half-transporters include a ~200-amino acid hydro-

* This work was supported by National Institutes of Health Grants R01HL071629, P41RR001395, and P01HL032262. The costs of publication of this article were defrayed in part by the payment of page charges. This article must therefore be hereby marked "*advertisement*" in accordance with 18 U.S.C. Section 1734 solely to indicate this fact.

¶ These authors contributed equally to this work.
‖ Recipient of a fellowship from the Gruss Lipper Foundation and the Marine Biological Laboratory.
** To whom correspondence should be addressed: Dept. of Pharmacology, Tufts University, Boston, MA 02111. Tel.: 617-636-3467; Fax: 617-636-6738; E-mail: orian.shirihai@tufts.edu.

[1] The abbreviations used are: ABC, ATP binding cassette; mTP, mitochondrial targeting presequence; EGFP, enhanced green fluorescence protein; ER, endoplasmic reticulum; TMRE, tetramethylrhodamine ethyl ester perchlorate; DFDNB, 1,5-difluoro-2,4-dinitrobenzene; MMCC, mean mitochondrial correlation coefficient.

philic ATP binding cassette and a ~400-amino acid hydrophobic transmembrane domain. Therefore, these proteins might present a challenge to mitochondrial import machinery. This study marks the first comprehensive analysis of the mitochondrial targeting, import, and assembly properties of an ABC transporter. We have previously reported on the murine mitochondrial transporter, ABCB10 (ABC-me). ABCB10 is induced during erythroid differentiation and is involved in heme biosynthesis (8). We report here that the ABCB10 preprotein includes an unusually long mTP of 105 residues that provides mitochondrial targeting redundancy and flexibility. Point mutation experiments reveal that ABCB10 additionally possesses downstream (aa 106–715) targeting signals capable of assisting a damaged mTP. To differentiate between protein trafficking and protein import, we combined confocal microscopy of living cells and biochemical analysis of isolated organelles. We show that removing part of the mTP of ABCB10 results in efficient trafficking but compromised import into the mitochondria. Quaternary structure analysis of ABCB10 indicates that it homo-oligomerizes in the mitochondrial inner membrane and does not appear to assemble with other proteins. ABCB10 that lacks its mTP is targeted not to mitochondria but to the ER, where it also oligomerizes.

EXPERIMENTAL PROCEDURES

Cell Culture and Transfection—HEK 293T and COS cells were cultured in low glucose DMEM without phenol red (Invitrogen) supplemented with 10% standard fetal bovine serum (Hyclone, Logan, UT), 2 mM L-glutamine (Invitrogen), and antibiotics at 37 °C in 5% CO_2, 95% air atmosphere. G1ER cells (24) were grown in Iscove's modified Dulbecco's medium (Invitrogen) supplemented with 15% heat-inactivated fetal calf serum, 2 units/ml Epoetin α (Amgen, Thousand Oaks, CA), 0.5% Chinese hamster ovary kit ligand (stem cell factor) conditioned medium (100 units/ml), and antibiotics. Transient transfections of HEK 293T cells and COS cells were performed using FuGene 6 (Roche Applied Science) according to the manufacturer's instructions. Cells were <15% confluent at transfection. Transfection efficiency was ~70%.

Plasmids and DNA Constructs—The 105-aa mTP of mouse ABCB10 and its five wild-type subdomains (aa 1–35, 36–70, 71–105, 1–70, and 36–105) were prepared by PCR using primers containing an EcoRI restriction site followed by a Kozak initiation sequence at the 5′-end and a BamHI restriction site at the 3′-end, using ABCB10 as template. Single amino acid mutations were performed by triple PCR, with multiple mutations achieved with additional rounds. Amplified fragments were digested and cloned into pEGFP-N1 vector (Clontech, Palo Alto, CA) with T4 DNA ligase (Roche Applied Science) using the EcoRI (5′) and BamHI (3′) restriction sites upstream to EGFP. Deletion constructs were also prepared by PCR. All constructs were validated by sequencing at the core facility at either Children's Hospital or Tufts University (Boston, MA).

Labeling of the Mitochondria and Endoplasmic Reticulum (ER), Confocal Microscopy, and Data Analysis—Mitochondria were labeled using the mitochondria-specific dyes tetramethylrhodamine ethyl ester perchlorate (TMRE) and Mitotracker Red CMH2Xros from Molecular Probes, Inc. (Eugene, OR). Freshly prepared TMRE was added to culture in Me_2SO (Fisher) at 50 nM and incubated for 10 min prior to visualization. Cells were kept in the dark and examined for a maximum of 15 min. Mitotracker Red was applied to culture at 100 nM, also in Me_2SO. The cells were incubated for 30 min and washed twice in warm culture medium. Mitotracker Red was used to verify the precise mitochondrial labeling of TMRE. The ER was labeled using the ER-specific dye ER-Tracker™ blue-white DPX (E-12353) at a concentration of 100 nM as directed by the manufacturer (Molecular Probes).

Confocal microscopy was performed on live cells in glass slide bottom dishes (MatTek, Ashland, MA) using a Zeiss LSM 510 Meta microscope with a × 63 oil immersion objective at 37 °C. Using multitrack analysis, red-emitting mitochondrial dyes were excited with a 543-nm helium/neon laser, and emission was recorded through a BP 650–710-nm filter. EGFP was excited using a 488-nm argon laser, and emission was recorded through a BP 500–550-nm filter. ER-Tracker blue-white DPX (E-12353) was excited with a two-photon laser, and emission was recorded through a BP 435–487-nm filter.

The correlation plot application of Metamorph image analysis software version 5.0 was employed for colocalization quantification and generation of scatter plots. 12–24 cells from a minimum of 8–12 colonies were analyzed per condition. Colocalization was analyzed for individual cells identified as regions of interest. They were averaged for each condition to determine a mean mitochondrial correlation coefficient (MMCC), and the S.E. was calculated. Relative significance of data sets was determined by a standard t test with the threshold set at $p < 0.05$.

Isolation of Mitochondria—Crude mitochondria were prepared by differential centrifugation as described (8). Density gradient purification was performed using OptiPrep™ as directed by the manufacturer (Axis-Shield, Oslo, Norway). The Bradford assay was used to spectrophotometrically determine the protein concentration using a NanoDrop ND-1000 UV-visible spectrophotometer (NanoDrop Technologies, Rockland, DE).

Protein Cross-linking and Immunoprecipitation—1,5-Difluoro-2,4-dinitrobenzene (DFDNB; Pierce) dissolved in Me_2SO was used as the cross-linking reagent at a concentration of 30 μg/30 μg of protein for low level and 300 μg/30 μg of protein for high level cross-linking. Gradient-purified mitochondria were suspended in 150 mM KCl and incubated in DFDNB at 0 °C for 30 min. The reaction was quenched at 25 °C for 30 s with 400 mM Tris base (pH 9). Cross-linking was also performed on whole cell lysate using a modified protocol in which the cells were resuspended in phosphate-buffered saline supplemented with Complete™ EDTA-free protease inhibitor (Roche Applied Science) and flash-frozen in liquid nitrogen to break the membranes. Cross-linking was performed as stated above, with the addition of 120 μg/ml DNase I (Roche Applied Science) during quenching. Immunoprecipitation was performed using Protein G-agarose beads (Roche Applied Science) and anti-V5 (1:500 dilution) (Invitrogen) and anti-c-Myc (1:500 dilution) (Invitrogen) antibodies as described (25).

One-dimensional SDS-PAGE, Silver Staining, and Western Blotting—Mitochondrial samples were taken up in sample buffer (62.5 mM Tris, 10% glycerol, 2% SDS, 1% Triton X-100, 2.5% β-mercaptoethanol, bromphenol blue), loaded on a 4–15% gradient Tris-HCl gel (Bio-Rad), and electrophoresed at 160 V in running buffer using a Bio-Rad Mini-Protean 3 cell. Proteins to be identified by MS/MS analysis were revealed by silver staining using the Silver Stain Plus kit (Bio-Rad).

For detection by Western blotting, proteins were transferred onto nitrocellulose or polyvinylidene difluoride membrane using a Bio-Rad TransBlot SD rapid transfer cell in Towbin buffer at 140 mA for 1 h at room temperature. Primary antibodies were anti-EGFP (1:2500 dilution) (Clontech) and anti-V5-horseradish peroxidase (1:5000 dilution) (Invitrogen). Protein was revealed using a Super Signal chemiluminescent horseradish peroxidase detection system as directed by the manufacturer (Pierce) and exposed to Kodak BioMax MR film (Eastman Kodak Co.).

Mass Spectrometry and N-terminal Sequencing—Protein identification of SDS-PAGE silver-stained bands was done by MS/MS analysis of tryptic peptides using the MS-fit program as previously described (26). N-terminal protein sequencing was performed by automated Edman degradation on an Applied Biosystems model 494 Procise sequencer. Samples separated by SDS-PAGE were transferred onto polyvinylidene difluoride membrane and stained with Coomassie Blue. Model 610A version 2.1 software was employed for data acquisition and processing.

Proteinase K Digestion of Extramitochondrial Proteins—Extramitochondrial protein digestion was carried out to verify complete mitochondrial insertion of each mTP and its passenger protein. It was performed on all constructs that targeted partially or entirely to mitochondria. Those constructs that targeted to mitochondria but were not fully imported are mentioned under "Results." To accomplish extramitochondrial protein digestion, gradient-purified mitochondria were incubated with 100 μg/ml proteinase K (Sigma) on ice for 30 min. Proteinase K was subsequently inactivated using a modified procedure described by Glick (27). Briefly, 2 mM phenylmethylsulfonyl fluoride (Pierce) was added, and the mitochondria were pelleted by centrifugation at 17,500 × g for 10 min at 4 °C. Mitochondria were resuspended in buffer C (0.6 M sorbitol (Fisher), 20 mM HEPES, pH 7.4) supplemented with 2× Complete™ protease inhibitor mixture (Roche Applied Science), 2 mM phenylmethylsulfonyl fluoride, and 5.5% (v/v) trichloroacetic acid (Sigma), heated to 70 °C for 5 min, and then incubated on ice for an additional 5 min. Mitochondria were reisolated by centrifugation at 12,000 × g for 10 min and immediately resuspended in sample buffer for separation by one-dimensional SDS-PAGE. 2 M Tris, pH 9, was added dropwise to neutralize the solution.

Whole Cell Protein Analysis—Whole cell protein analysis was performed to control for post-translational stability of transfected constructs. The procedure was carried out on all constructs that did not target to mitochondria. Those constructs that were cleaved prior to mitochondrial targeting, thus reducing targeting efficiency, are men-

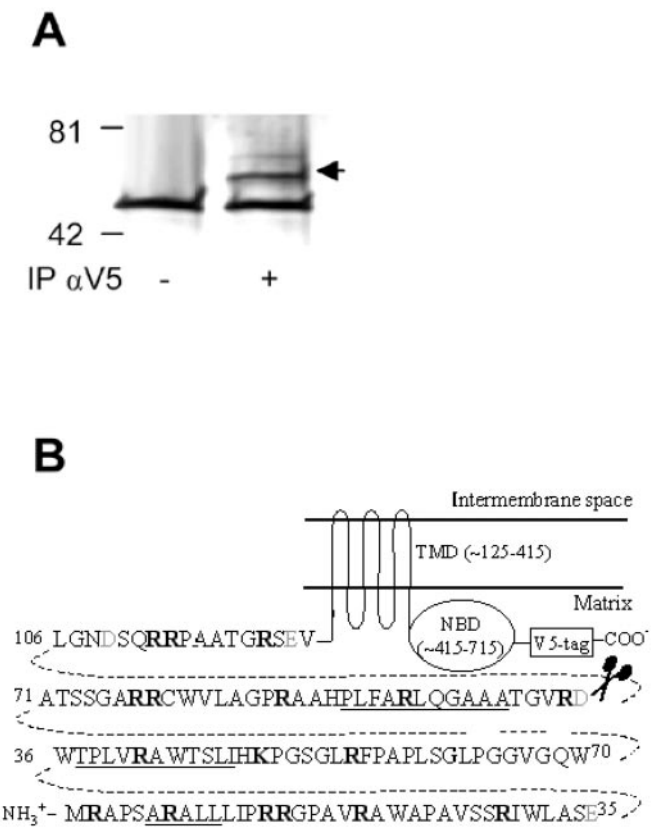

FIG. 1. **The mTP of ABCB10.** *A*, silver stain of immunoprecipitated ABCB10 isolated from mitochondria of HEK 293T cells transfected with ABCB10-V5. *Lane 1*, negative control of immunoprecipitation (*IP*) using anti-c-Myc antibody. *Lane 2*, immunoprecipitation using anti-V5 antibody. A band (verified as ABCB10-V5 by mass spectrometry) appears at ~65 kDa (indicated by an *arrow*). An artifact of immunoprecipitation appears in both *lanes* at ~55 kDa. ABCB10-V5 was excised from the gel and subjected to N-terminal sequencing. *B*, the first 123 amino acids of ABCB10 and the position of the protein in the mitochondria. N-terminal sequencing of mature protein identified the first 17 amino acids as LGNDSQRRPAATGRSEV, corresponding to Leu^{106}–Val^{123}, indicating that the mTP is composed of aa 1–105. Basic residues are in *boldface type*, and acidic residues are in *gray*. Predicted α-helices are *underlined*. Note that the hydrophobic transmembrane domain (*TMD*) and hydrophilic nucleotide binding domain (*NBD*) each represent large fractions of the imported protein.

tioned under "Results." For whole cell protein analysis, cells were lysed in buffer C, supplemented with 0.1% (v/v) SDS and 2 μM pepstatin A (Roche Applied Science) to prevent protein degradation. Protein was then precipitated using 5.5% (v/v) trichloroacetic acid and immediately separated by SDS-PAGE.

RESULTS

Identification of ABCB10 Presequence Cleavage Site—ABCB10 fused to V5 at its C-terminal was expressed in HEK 293T cells, immunoprecipitated, and separated by SDS-PAGE. Silver staining revealed a band at ~65 kDa (Fig. 1*A*). This band was subjected to tryptic fragment analysis by tandem mass spectrometry and was identified as ABCB10, with the fragments obtained indicating that a larger than expected portion of the N terminus could be missing (data not shown). N-terminal sequencing performed on the band identified the first 17 amino acids as LGNDSQRRPAATGRSEV, which correspond to ABCB10 aa 106–123 (Fig. 1*B*). The 105-aa mTP of ABCB10 is unusually long compared with the mean mTP length of 34 residues ± 17 (one S.D.) (28).

The mTP of ABCB10 Is Necessary for Mitochondrial Import of ABCB10 and Sufficient for Import of EGFP—To explore the mitochondrial targeting and import properties of ABCB10 and its mTP, EGFP was fused at their C termini, and the proteins were expressed in HEK 293T cells. Their colocalization with mitochondria stained with TMRE was analyzed by confocal microscopy (Fig. 2). Metamorph image analysis software generated per-pixel scatter plots of red and green signal intensities. The MMCC is a measure of the scatter plot's tendency for positive linear correlation. Thus, a value of +1 represents perfect mitochondrial colocalization, 0 represents no mitochondrial preference, and −1 represents perfect mitochondrial exclusion. Since HEK 293T fibroblasts grow in adherent colonies, cells were selected from at least 12 colonies to minimize the impact of clonal variation. EGFP has been employed previously for similar subcellular localization studies (18, 29). EGFP alone is cytosolically localized and shows no organellar preference (Fig. 2*E*). EGFP carries consecutive negative charges at residues 6E and 7E of the EGFP molecule. Concentrated negative charge is highly unfavorable to mitochondrial targeting (16). Therefore, it is believed that C-terminal EGFP fusion does not enhance mitochondrial targeting of a molecule.

As expected, ABCB10-EGFP co-localizes with mitochondria, giving an MMCC of 0.81 ± 0.02 (Fig. 2*A*). The mTP of ABCB10 alone also targets EGFP to the mitochondria, demonstrating its sufficiency as an mTP. The MMCC for aa 1–105-EGFP is 0.81 ± 0.02 (Fig. 2*B*). To ensure that these proteins were fully imported into mitochondria, in addition to their being trafficked to the mitochondrial surface, biochemical analysis of their position was performed. Density gradient-purified mitochondria were isolated from HEK 293T expressing the protein of interest. Mitochondria were then subjected to proteinase K digestion of extramitochondrial proteins, and the results were analyzed by Western blotting. Western blots of aa 1–105-EGFP pre- and postdigestion were identical, indicating that complete import was accomplished (data not shown). This validation procedure was carried out on all subsequently examined constructs that targeted to mitochondria (see "Experimental Procedures").

Removal of the mTP from ABCB10-EGFP drastically reduces mitochondrial targeting, resulting in an MMCC of Δ105-ABCB10-EGFP of 0.33 ± 0.03 (Fig. 2*C*). For experimental control, mitochondrial targeting was additionally calculated for EGFP C-terminally fused to a standard, commercially available mTP, subunit VIII of human cytochrome *c* oxidase (Clontech), and EGFP alone (Fig. 2, *D* and *E*). The negative MMCC for EGFP alone indicates that it avoids mitochondria. To ensure that the failure of Δ105-ABCB10-EGFP to target to mitochondria was not due to post-translational cleavage, cell lysate was prepared and analyzed by Western blotting with anti-EGFP. All Δ105-ABCB10-EGFP that was detected appeared at an apparent molecular weight consistent with the predicted value (data not shown). This procedure was carried out on all subsequently examined constructs that failed to efficiently target to mitochondria (see "Experimental Procedures").

Removal of the mTP Results in the Mistargeting of ABCB10 to the ER—Δ105-ABCB10-EGFP does not appear ubiquitously in the cytoplasm but rather is identified as a meshlike structure characteristic of the ER membrane (Fig. 2*C*). Cells expressing Δ105-ABCB10-EGFP were co-stained with the ER-specific dye ER-Tracker blue-white DPX (E-12353) and subjected to ER colocalization quantification according to the same technique as mitochondrial colocalization (Fig. 2*F*). Δ105-ABCB10-EGFP is targeted into the ER with high efficiency, suggesting that an alternative subcellular distribution of ABCB10 or isoforms of ABCB10 may exist. Subcellular localization of Δ105-ABCB10 was additionally examined in COS cells, yielding identical ER preference (data not shown).

Fragmentation of the mTP of ABCB10 and Identification of a Critical Targeting Region—The primary amino acid sequence

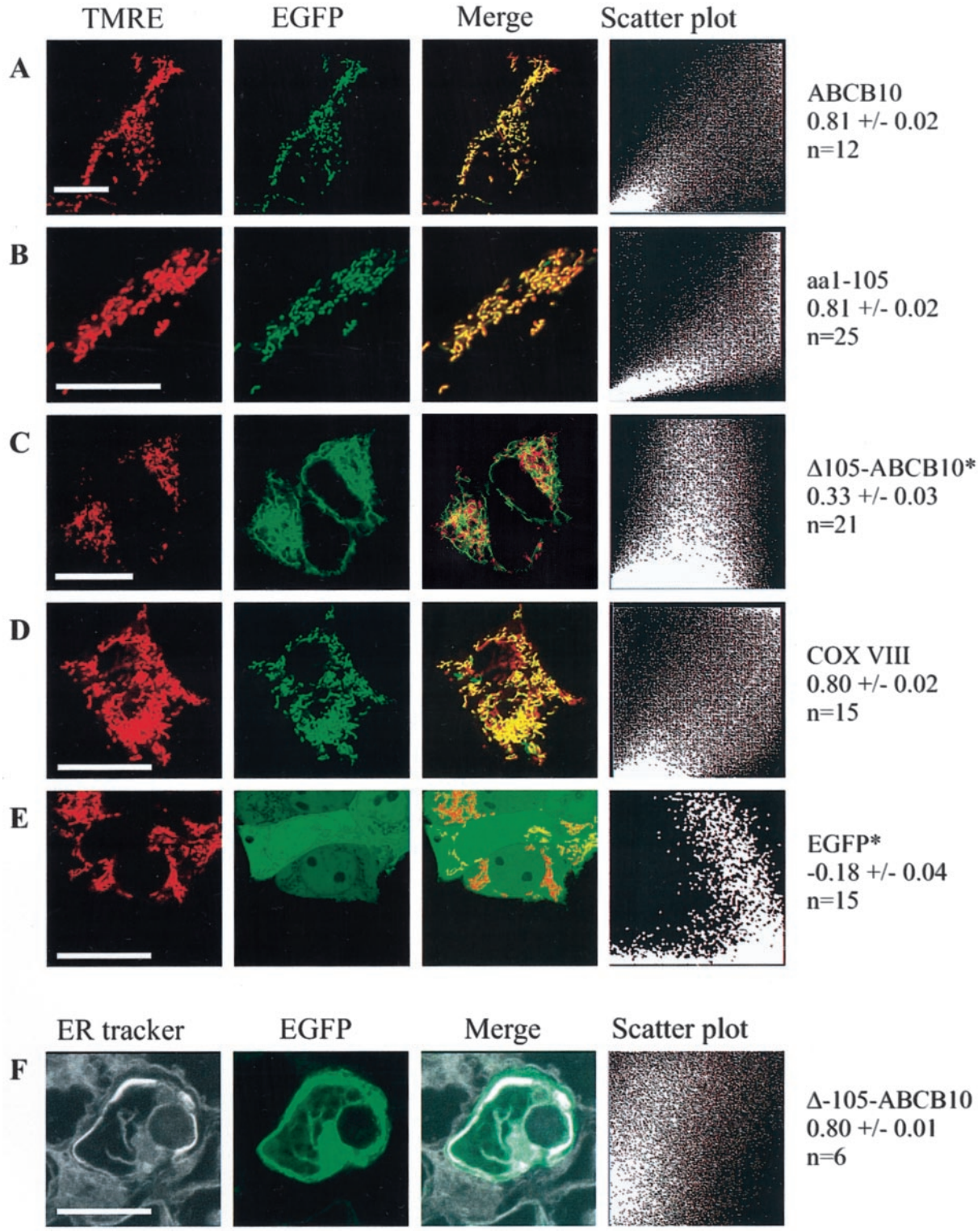

FIG. 2. **The 105-aa mTP of ABCB10 is sufficient and necessary to import ABCB10-EGFP into mitochondria.** Confocal microscopy of EGFP colocalization with mitochondria was used to analyze the mitochondrial targeting of ABCB10 and its mTP. *Red*, TMRE, a mitochondria-specific dye; *green*, EGFP, which is fused to the C-terminals of all constructs. Colocalization appears *yellow* and *orange* in the merged frames. Scatter plots plot each pixel according to its *green* and *red* intensities, *green* on the *x* axis and *red* on the *y* axis. MMCC was calculated for each construct using 12–24 cells. Proteins that target to mitochondria at significantly lower efficiency than wild-type ABCB10 are indicated with an *asterisk*. Representative cells are displayed. *Bars*, 20 μm. *A*, wild-type ABCB10; excellent mitochondrial targeting. *B*, mTP alone is sufficient for mitochondrial targeting. *C*, Δ105-ABCB10 is not targeted to mitochondria but rather to an alternate structure. *D*, positive control; EGFP fused to the commercially available mTP of COXVIII. *E*, negative control; EGFP lacking a targeting peptide is ubiquitously distributed throughout the cell. *F*, Δ105-ABCB10 colocalizes well with ER-tracker dye (*white*); scatter plot displays *green* on the *x* axis and *white* on the *y* axis.

(Fig. 1*B*) and predicted secondary structure of the mTP of ABCB10 were examined for features characteristic of mTPs. The distribution of both positive charge and hydrophobic moment (a measure of amphiphilicity) along the mTP of ABCB10 follows a pattern that delineates three distinct subdomains (Fig. 3, *A* and *B*). Similarly, the three putative α-helices are

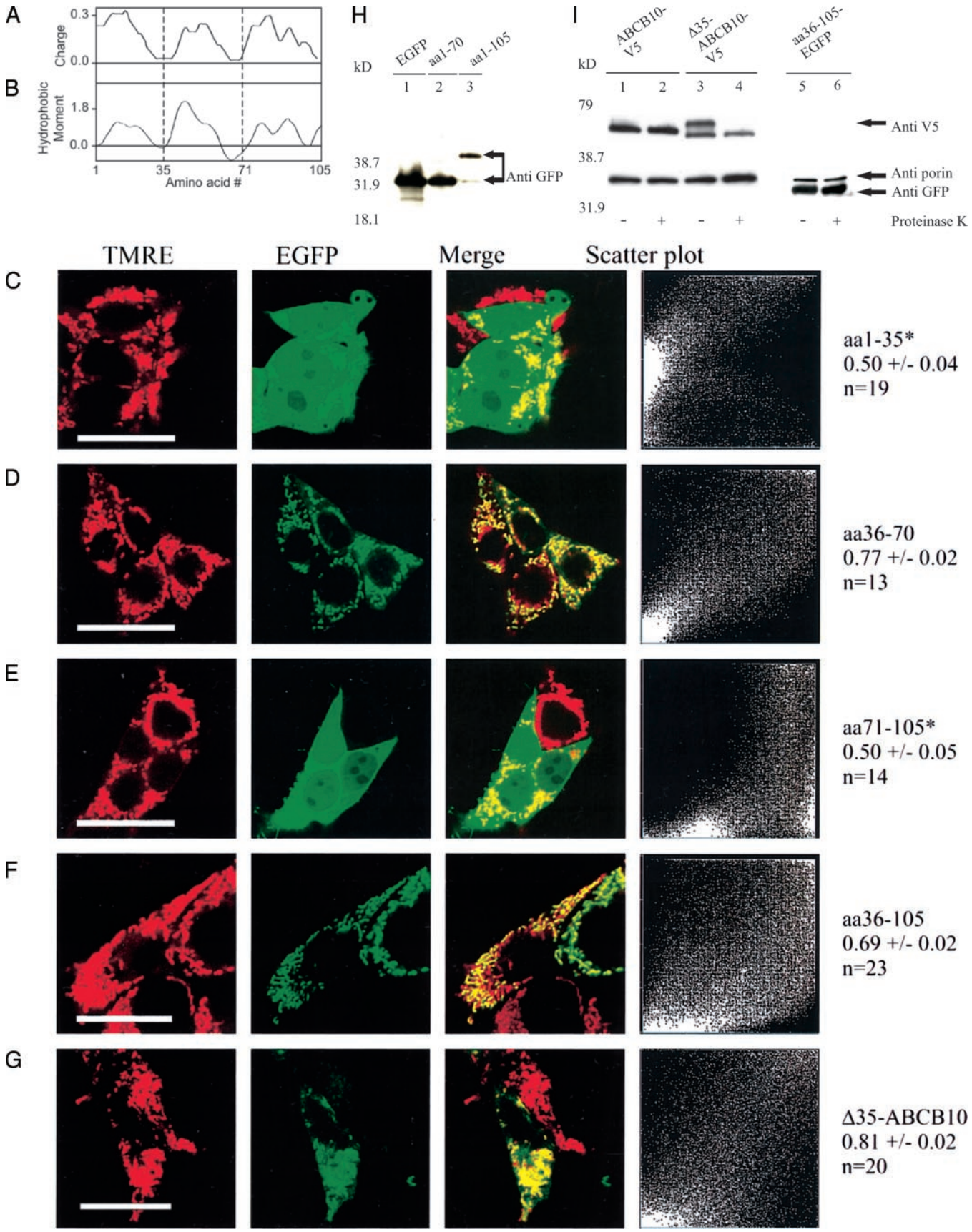

FIG. 3. **Targeting of the subdomains of the mTP of ABCB10 and role of aa 1–35 in mitochondrial import of ABCB10.** *A*, plot of charge distribution along the mTP of ABCB10. A sliding window of 12 aa was used to calculate average charge. *B*, hydrophobic moment plot of the mTP calculated according to Eisenberg's algorithm using a δ-angle of 100° and a consensus hydrophobicity scale, a measure of amphiphilicity. Note the presence of three regions of the mTP, each containing a maximum in positive charge, a peak in hydrophobic moment, and a single predicted α-helix. *C–E*, the central subdomain is as effective at targeting EGFP to mitochondria as the entire mTP. aa 1–35 and 71–105 demonstrate reduced mitochondrial targeting compared with the entire mTP. An *asterisk* indicates significant difference. *F* and *G*, removal of aa 1–35 from the mTP and

dispersed one per subdomain (Fig. 1*B*). To investigate underlying independent functionality of the three subdomains, fragmentation and mutation experiments were performed. The mTP was divided into three 35-aa fragments: aa 1–35, 36–70, and 71–105. The two negatively charged residues of the mTP of ABCB10 are located in positions 35 and 105, the C-terminal residues on the first and third fragments, respectively. Their proximity to EGFP minimizes their effect on the targeting properties of the mTP. Since the average length of all confirmed mTPs is 34 aa, the targeting efficiency of the fragments is not compromised by mTP length alone (28). Thus, examination of the targeting of the mTP fragments offers insight into the inherent properties in each region.

The central 35 aa of the mTP of ABCB10 is more effective at targeting EGFP to mitochondria than the flanking subdomains (Fig. 3). aa 1–35 and 71–105 only partially target EGFP to the mitochondria (MMCC of 0.50 ± 0.04 and 0.50 ± 0.05, respectively). aa 36–70 targets EGFP to the mitochondria as efficiently as the entire mTP of ABCB10 (Figs. 2*B* and 3*D*). aa 1–70, which is expected to target to mitochondria well, has a low MMCC of 0.27 ± 0.05 (data not shown). However, Western blot analysis of cell lysate found that the protein is unstable (Fig. 3*H*). Ambiguous cleavage events free EGFP from the rest of the protein, thereby causing EGFP to localize to the cytoplasm. A similar process occurred when aa 36–70 alone was N-terminally fused to Δ105-ABCB10-EGFP to determine the capacity of the isolated central subdomain of the mTP to target ABCB10 to the mitochondria. The resulting protein was unstable in both HEK 293T cells and COS cells (data not shown).

Functional Analysis of aa 1–35: Evidence for a Role in the Translocation of ABCB10 across Mitochondrial Membranes—The N-terminal subdomain of the mTP, aa 1–35, is not essential for the trafficking of ABCB10 to mitochondria. Both aa 36–105-EGFP and Δ35-ABCB10-EGFP are brought to the mitochondrial surface (Fig. 3, *F* and *G*). Western blot analysis suggested, however, that Δ35-ABCB10-V5 is not fully inserted into mitochondria despite reaching their outer membranes. Western blot analysis of density gradient-purified mitochondria was carried out on cells expressing either ABCB10-V5 or Δ35-ABCB10-V5. Wild-type ABCB10-V5 appears as a major band corresponding to the molecular weight of the mature protein from which the mTP has been cleaved (Fig. 3*I*). When SDS-PAGE is performed within 24 h post-transfection, a faint, higher molecular weight band corresponding to the approximate weight of the immature, uncleaved protein is present (as seen in Fig. 1*A*). Δ35-ABCB10-V5 appears as two bands of nearly equal strength, indicating that a substantial fraction of the protein is left uncleaved. Since mitochondrial presequences are known to be cleaved by enzymes located in the mitochondrial matrix, significant amounts of Δ35-ABCB10-V5 probably fail to translocate across both mitochondrial membranes. Extramitochondrial protein digestion by proteinase K performed on isolated mitochondria results in the complete disappearance of the high molecular weight Δ35-ABCB10-V5 band and leaves the low molecular weight Δ35-ABCB10-V5 band unchanged, supporting the role of aa 1–35 in the mitochondrial import of ABCB10 into the inner membrane. Unlike Δ35-ABCB10-V5, aa 36–105-EGFP does not significantly degrade in the presence of proteinase K. This suggests that full mitochondrial insertion and proper presequence cleavage takes place. Therefore, the downstream domain of ABCB10 (aa 106–715) appears to present a challenge to mitochondrial import machinery not found in EGFP alone. Although not essential for efficient mitochondrial targeting, aa 1–35 is required for proper mitochondrial insertion.

TABLE I

Recognized features of mTPs are not essential components of aa 36–70

Mutating neither arginine residues (alone or in tandem) nor the predicted α-helix significantly reduces the mitochondrial targeting of aa 36–70.

Mutation	MMCC	*n*
Wild type	0.77 ± 0.02	12
aa 36–70-R41A	0.71 ± 0.04	12
aa 36–70-R55A	0.76 ± 0.03	12
aa 36–70-R41A-R55A	0.74 ± 0.03	28
aa 36–70-R41P	0.73 ± 0.02	19
aa 36–70-A42P	0.75 ± 0.03	16

Identification of Elements of the mTP Essential for Mitochondrial Targeting—A series of specific amino acid mutation experiments were performed to elucidate the features of aa 36–70 that are necessary for its mitochondrial targeting. Mutations directed at removing arginine residues, disrupting the predicted α-helix, and replacing hydrophobic residues were carried out. aa 36–70 contains two arginine residues at positions 41 and 55, and these were mutated to alanine individually and in tandem. Alanine possesses similar helix formation properties to arginine, thereby limiting the effect of arginine replacement to removing its positive charge. All three mutants, R41A, R55A, and R41A/R55A, targeted EGFP to mitochondria nearly as efficiently as wild-type: MMCC values of 0.71 ± 0.04, 0.76 ± 0.03, and 0.74 ± 0.03, respectively (Table I). This was surprising in light of the presumed importance of arginine in mTPs. aa 36–70 effectively targets EGFP to the mitochondria with no arginine residues and a single positively charged residue, Lys^{49}.

To test the importance of the region's α-helix, the secondary structure of aa 36–70 was disrupted. The predicted α-helix of aa 36–70 falls at aa 37–47. Mutating either Ala^{42} to Pro or Arg^{41} to Pro is expected to destroy this conformation. Both mutations were carried out, and neither significantly reduced the mitochondrial targeting efficiency (Table I). The mTP of ABCB10 therefore does not require a predictable α-helix for normal mitochondrial targeting.

The aa 36–70 fragment possesses considerable hydrophobic character. We removed one hydrophobic residue pair with the double mutation L46Q/I47Q. Glutamine residues were substituted for leucine and isoleucine to maintain the helix formation and neutral charge properties of wild type. This mutation resulted in drastic reduction in mitochondrial targeting of aa 36–70: MMCC = 0.30 ± 0.06 (Fig. 4*A*). The mitochondrial targeting efficiency of aa 36–70 was reduced significantly further with the addition of the R41A mutation (MMCC = 0.15 ± 0.02), indicating that a threshold was breached that prevents the ability of mTP to overcome the mutation of Arg^{41} (Fig. 4*B*).

The Addition of aa 1–35 and 71–105 to Hydrophobically Mutated aa 36–70 Fails to Fully Rescue Mitochondrial Target-

ABCB10 does not significantly reduce mitochondrial targeting of either protein compared with wild-type mTP and wild-type ABCB10, respectively. *Bars* in *C–G*, 20 μm. *H*, Western blot of protein isolated from whole HEK 293T cells expressing EGFP alone (*lane 1*), aa 1–70-EGFP (*lane 2*), and aa 1–105-EGFP (*lane 3*). Cleavage of EGFP occurs from aa 1–70-EGFP but not from aa 1–105-EGFP. *I*, Western blot of density gradient purified mitochondria isolated from HEK 293T cells expressing ABCB10-V5 (*lanes 1* and *2*), Δ35-ABCB10-V5 (*lanes 3* and 4), or aa 36–105-EGFP (*lanes 5* and *6*). The high molecular weight band in L3 is thought to be uncleaved protein, suggesting that the preprotein of Δ35-ABCB10-V5 did not reach the mitochondrial matrix. Digestion of extramitochondrial proteins by proteinase K corroborates this finding. Of the three proteins, only Δ35-ABCB10-V5 is incompletely imported into the mitochondria. Loading of protein and localization of proteinase activity are controlled by probing for porin, an abundant mitochondrial outer membrane protein. *GFP*, green fluorescent protein.

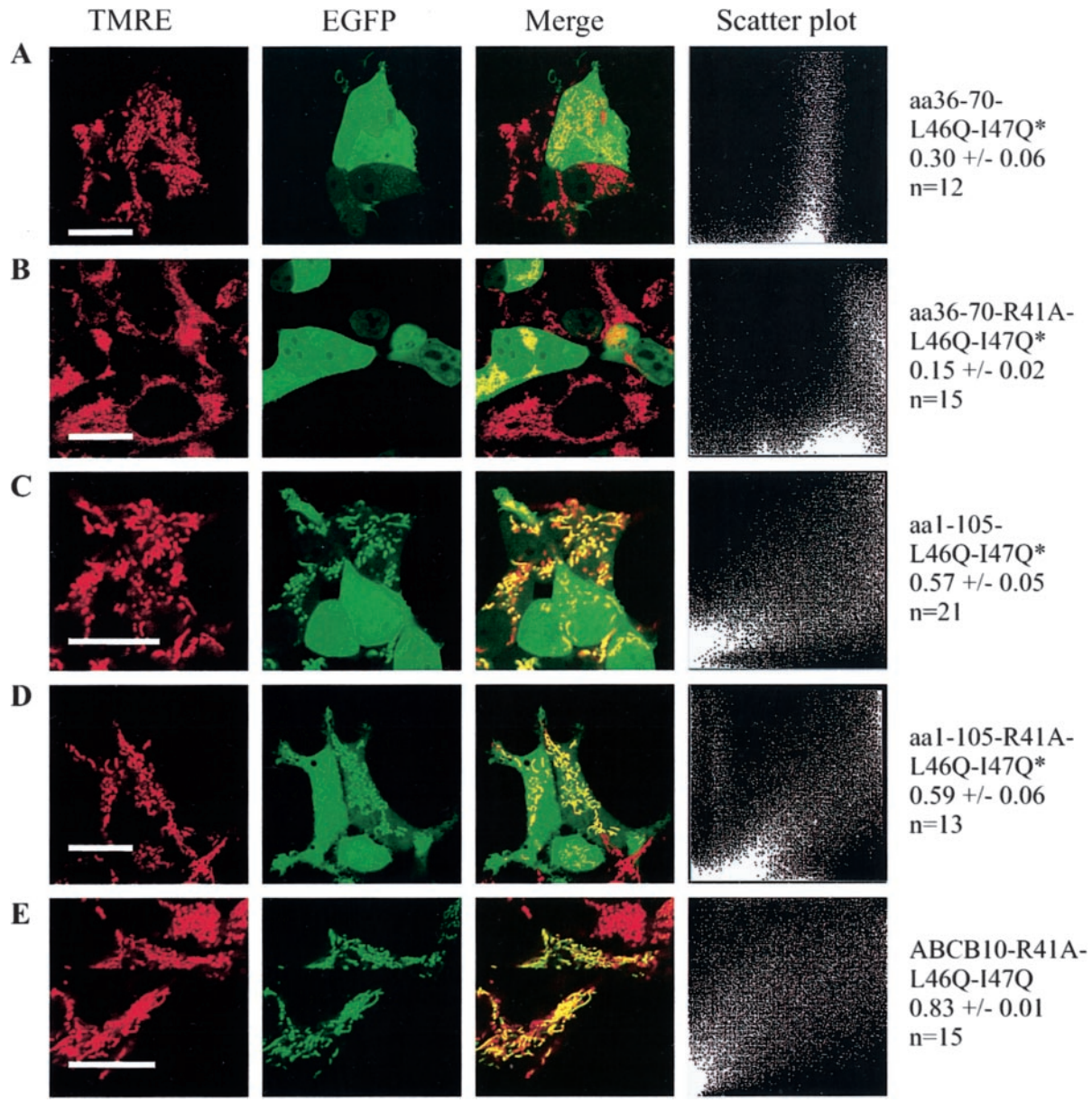

FIG. 4. **Mutating mitochondrial targeting elements of aa 1–35 identifies essential hydrophobic residues.** *A*, mutating hydrophobic residues Leu[46]-Ile[47] significantly reduces mitochondrial targeting of aa 36–70 compared with wild type. *B*, the L46Q/I47Q mutant is additionally susceptible to reduction of targeting efficiency by R41A mutation. The *asterisk* indicates significant difference from aa 36–70-L46Q/I47Q. *C* and *D*, rejoining aa 1–35 and 71–105 to aa 36–70-L46Q/I47Q and aa 36–70-L46Q/I47Q/R41A partially restores mitochondrial targeting. The *asterisks* indicate significant difference from mitochondrial targeting of wild-type aa 1–105. Therefore, rescue is incomplete. *E*, fusing aa 106–715 to aa 1–105-L46Q/I47Q/R41A restores mitochondrial targeting to that of wild-type ABCB10. *Bars*, 20 μm.

ing—The flanking thirds of the mTP, aa 1–35 and 71–105, only partially rescue the effect of the L46Q/I47Q mutations on aa 36–70, demonstrating that the Leu[46]-Ile[47] hydrophobic pair of the mTP of ABCB10 is essential for its mitochondrial targeting (Fig. 4*C*). Since additional mutation of Arg[41] to Ala in the hydrophobic mutant results in no further decrease in mitochondrial targeting, the importance of the R41A mutation observed in the aa 36–70 hydrophobic mutant is negated by the presence of the flanking regions (Fig. 4, *B* and *D*).

Downstream (aa 106–715) Elements of ABCB10 Rescue Impaired Targeting of Mutated mTP—The internal domain of ABCB10 (aa 106–715) completely restores mitochondrial targeting of the mutated mTP. The R41A/L46Q/I47Q mutations were carried out in full-length ABCB10 (715 aa) fused to EGFP (Fig. 4*E*). The protein targeted to mitochondria as efficiently as wild-type and at a significantly greater level than the mutated 105-aa mTP alone. Thus, internal regions of ABCB10, in addition to the mTP, possess mitochondrial targeting information.

ABCB10 Oligomerizes in the Inner Membrane—The membrane-permeable cross-linker DFDNB was used to cross-link endogenous ABCB10 in mitochondria isolated from differentiating erythroid cells and V5 epitope-tagged ABCB10 in HEK 293T cells. When DFDNB was added, a band at ~130 kDa, the approximate mass of an ABCB10 homodimer, appeared and strengthened in intensity with increasing amounts of DFDNB over the range of 0.1–10 mg/mg of protein (Fig. 5*A*). The band at ~65 kDa weakened with more DFDNB. The ~130-kDa band similarly appeared when the mitochondrial preparation expressing ABCB10-V5 was run on SDS-PAGE in the absence of β-mercaptoethanol (Fig. 5*B*). A higher molecular mass band (>200 kDa) also appeared with cross-linking, its intensity similarly related to the concentration of DFDNB.

ABCB10 Forms Homodimers and Homo-oligomers—To determine whether the ABCB10 complexes include ABCB10 ho-

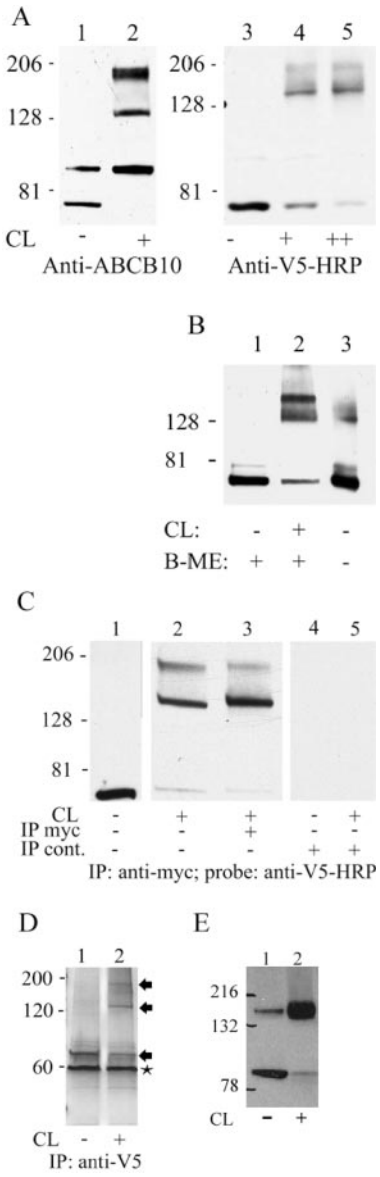

FIG. 5. **Quaternary structure assembly of ABCB10.** *A*, *lanes 1* and *2*, Western blot of mitochondria isolated from wild-type G1ER cells, in the absence (*lane 1*) and presence (*lane 2*) of cross-linker DFDNB (*CL*), probed with anti-ABCB10. The ABCB10 monomer at ~65 kDa diminishes in the presence of DFDNB, and a new band at ~130 kDa appears. The band at ~95 kDa is a cross-reactivity artifact of this antibody. Note that this artifact is unaffected by DFDNB, demonstrating the cross-linker's specificity. *Lanes 3–5*, Western blot of mitochondria harvested from HEK 293T cells expressing V5-tagged ABCB10 and probed with anti-V5-horseradish peroxidase (*HRP*) antibody. Increasing DFDNB concentration from 0.1 mg/mg of protein (*lane 4*) to 10 mg/mg of protein (*lane 5*) results in more complete cross-linking of ABCB10 monomers. *B*, Western blot of mitochondria isolated from HEK 293T cells expressing ABCB10-V5. SDS-PAGE in the absence of reducing agent β-mercaptoethanol (*B-ME*; *lane 2*) preserves higher molecular weight ABCB10 complexes. *C*, Western blot of mitochondria harvested from HEK 293T cells co-transfected with ABCB10-V5 and ABCB10-c-Myc. Detection using anti-V5-horseradish peroxidase followed chemical cross-linking by DFDNB and immunoprecipitation (*IP*) with anti-c-Myc. Control for immunoprecipitation (*lanes 4* and *5*) used antibody-free serum in place of anti-c-Myc antibody. *D*, silver stain of immunoprecipitated ABCB10-V5 from control (*lane 1*) and cross-linked (*lane 2*) mitochondria of HEK 293T cells. Bands in *lane 2* marked with *arrowheads* were excised and identified using MS/MS tryptic fragment analysis. The *star-marked band* at ~60 kDa is an artifact of the anti-V5 antibody used for immunoprecipitation. *E*, Western blot of whole cell protein isolated from HEK 293T cells transfected with Δ105-ABCB10-V5. The addition of DFDNB (*lane 2*) results in a shift of monomeric ABCB10 to complexes consistent in weight with homodimers of ABCB10.

modimers, HEK 293T cells were double transfected with both V5 and c-Myc-tagged ABCB10. After isolating the mitochondria and cross-linking as above, ABCB10 was immunoprecipitated using anti-c-Myc antibody. The precipitated proteins were separated by SDS-PAGE and Western blotted using horseradish peroxidase-conjugated anti-V5 antibody. Bands appeared at ~65 and ~130 kDa (Fig. 5*C*). This demonstrates that both ABCB10 species, the c-Myc-tagged and the V5-tagged, were components of some of the cross-linked complexes and indicates that ABCB10 forms homodimers. The band at ~65 kDa revealed that some ABCB10 complexes that had not been cross-linked nevertheless co-immunoprecipitated intact and ultimately were separated during SDS-PAGE. The anti-c-Myc antibody was replaced with rabbit serum to verify immunoprecipitation specificity. Immunoprecipitated ABCB10-V5 from control and cross-linked samples were additionally probed with silver stain (Fig. 5*D*). All bands identified under cross-linking conditions (*arrowheads*) were subjected to MS/MS tryptic fragment analysis. Only ABCB10 was identified in all bands, suggesting that ABCB10 homo-oligomerizes and that no other protein takes part in its quaternary structure assembly.

ER-targeted ABCB10 Forms Dimers—The quaternary structure assembly partners of ER-localized Δ105-ABCB10-EGFP were examined in similar fashion. Cross-linking by DFDNB and Western blotting was performed on whole cell lysates (Fig. 5*E*). Δ105-ABCB10-V5 appears to assemble into complexes identical to those observed for wild-type ABCB10-V5. Thus, the homodimerization of ABCB10 observed in mitochondria is neither organelle-specific nor mTP-dependent.

DISCUSSION

Mitochondrial ABC transporters play a key role in iron metabolism and heme biosynthesis. Consisting of hydrophobic as well as hydrophilic domains, ABC transporters may present a challenge to mitochondrial import machinery. Four mammalian mitochondrial transporters besides ABCB10 have been discovered: ABC7, M-ABC1, M-ABC2, and MTABC3. ABC7, M-ABC2, and M-ABC1 have been shown to possess mTPs (12, 30, 31). Computational analysis of MTABC3 predicts that it does not possess an mTP and therefore is likely to enter the mitochondrion via the Tom70 pathway. All mitochondrial ABC transporters described to date are of the half-transporter type and therefore predicted to dimerize; however, their dimerization partners have not yet been identified. We report here the first comprehensive analysis and characterization of the import of a mitochondrial ABC transporter, ABCB10, and its assembly into a homodimer in the inner membrane. We applied combined microscopy and cellular fractionation to study the function of different components of the mTP in trafficking, import, and dimerization of ABCB10. Taking this approach, we show that whereas the middle segment of the mTP contains hydrophobic residues essential for trafficking of the protein to the organelle, the N-terminal subdomain is necessary for proper insertion of the protein into the organelle. Further, we show that ABCB10 homodimerizes in the inner membrane and can similarly assemble into dimers in the ER when expressed without the mTP.

We determined that the mTP of ABCB10 is sufficient for mitochondrial import of EGFP and that the middle fragment (aa 36–70) contains the minimal information necessary to direct these processes. Net positive charge, derived particularly from arginine residues, and amphiphilic α-helices are thought to play important roles in the mitochondrial targeting properties of mTPs (14, 17). Removal of these elements by mutation in aa 36–70-EGFP results in wild-type phenotype. We therefore speculate that certain mTPs possess flexible and redundant mitochondrial targeting properties that allow

them to bypass the use of conventional targeting mechanisms. Further mutation experiments identified two key hydrophobic residues that are essential for efficient mitochondrial targeting. A hydrophobic pentapeptide motif has been identified as essential for recognition by the TOM complex both *in vitro* and *in vivo* (18, 19). This motif occurs three times in aa 36–70, one of which includes Leu^{46}-Ile^{47}. Mutating these residues to glutamine destroyed most of the mitochondrial targeting of aa 36–70 and left the peptide susceptible to additional reduction in targeting efficiency by arginine replacement. This indicates that, like plant F_1-ATP synthase (18), ABCB10 associates with Tom20 via hydrophobic interactions, as described by Abe *et al.* (32). Fusing the flanking regions of the mTP to aa 36–70 failed to completely rescue the effect rendered by the hydrophobic mutations yet did attenuate the additional insult imparted by the R41A mutation. This suggests that the distribution of positive charge in the mTP of ABCB10 has margin for error, supporting its role as a provider of thermodynamic energy for translocation and not for precise recognition and binding with import machinery (33). On the contrary, the hydrophobic residues responsible for Tom20 interaction must meet stringent accessibility and location requirements, since all nine additional hydrophobic pentapeptide motifs of the aforementioned type introduced by the flanking regions failed to completely rescue the L46Q/I47Q mutation. Fusion of the internal region of ABCB10, aa 106–715, to the hydrophobically mutated 105-aa mTP fully rescued mitochondrial targeting. This implies that ABCB10 contains internal signals that provide targeting information in addition to the mTP. This has been observed in the inner membrane protein cytochrome c1 but is a relatively rare feature of nuclear encoded mitochondrial proteins (34). Although the hydrophobically mutated mTP and the internal domain independently are incapable of targeting EGFP to the mitochondria, their union creates an efficiently targeted protein (without the introduction of a necessary targeting element at their junction). A similar phenomenon was demonstrated by Galanis *et al.* (35), who by doubling a mitochondrial presequence increased its targeting potency. Considering the challenge to mitochondrial import that ABCB10 presents, the protein is an ideal candidate for possessing redundant import features.

To determine whether aa 1–35 improves mitochondrial targeting by providing additive information to the targeting properties of aa 36–70, aa 1–70-EGFP was constructed; however, the resulting protein was unstable. This demonstrates the potential instability of EGFP-tagged proteins and the necessity to verify that unanticipated cleavage does not occur. Instead, we assessed the effect that the absence of aa 1–35 had on targeting efficiency by constructing Δ35-ABCB10-EGFP/V5. Fluorescence microscopy found that the absence of aa 1–35 does not significantly reduce mitochondrial targeting of ABCB10-EGFP. However, proteinase K digestion of extramitochondrial proteins found that translocation of Δ35-ABCB10-V5 across the mitochondrial membrane is reduced, indicating that the processes of mitochondrial targeting and import can be separated. aa 1–35, although necessary for proper mitochondrial import of ABCB10-V5, is not required for that of EGFP, a purely hydrophilic protein. Thus, the distinction between mitochondrial trafficking and import may be more easily observed in proteins that challenge the trafficking/import machinery. The mechanism by which aa 1–35 directs the mitochondrial import of ABCB10 is potentially related to a number of characteristics of ABCB10 and the import machinery. Since mitochondrial proteins are predicted to enter the mitochondria either through a linear or loop conformation, depending on the import pathway, aa 1–35 may affect the folding of ABCB10 and thereby influence the pathway selected (13, 36). Since each mitochondrial membrane possesses its unique import machinery, aa 1–35 may be specifically required for import across the inner membrane but not the outer. Mislocalization of imported proteins among the mitochondrial compartments has been demonstrated in cytochrome *c* oxidase subunit Va (37). Alternatively, aa 1–35 might simply add import elements needed to overcome a threshold, similar to the additive targeting properties observed in ABCB10. Further investigation will help to tease apart mitochondrial trafficking and import mechanisms and explain the obstacles that ABCB10 presents to each.

ABCB10 lacking its 105-aa mTP efficiently localizes to the ER, raising the possibility that an isoform of ABCB10 is present in the ER under physiological conditions or when the start codon is mutated. A number of proteins have been described that employ alternate splicing or post-translational modification to direct ER or mitochondria-specific targeting as required. cAMP-dependent phosphorylation orchestrates the redirection of cytochromes to either the ER or mitochondria in response to cellular signaling cascades (38). Alternate splicing of D-AKAP1 results in its tissue-specific localization in either the ER or the mitochondria (29). Similarly, use of an alternate transcriptional start site for cytochrome P450 monooxygenase redirects this predominantly ER protein to mitochondria in the liver and extrahepatic tissues (39). Although alternative splice variants of ABCB10 have not yet been identified, the availability of additional, in-frame transcriptional start sites at amino acid positions 151 and 201 and preliminary 5′ RACE results (data not shown) lead us to suspect their presence. Computational analysis (Target P and PSORTII) of the targeting properties of the putative secondary start site isoform strongly predicts ER localization. With time (>24 h) after transfection of Δ105-ABCB10-EGFP, the ER undergoes morphological change. Studies by van Leeuwen *et al.* (40) suggest that ER stress may result from a mistargeted protein functioning in the ER. Depletion or accumulation of substrate within the ER by ABCB10 could cause damage to the organelle. This would imply that ABCB10 is functional in the ER, is oriented in a consistent fashion, and exists with any necessary assembly partners.

ABCB10 is of the half-transporter type as described by Higgins (1). Dimerization of ABC half-transporters has been shown to be necessary to achieve functionality (6, 41) and has been observed in many ABC proteins. Homodimerization has been observed in ABC transporters of the plasma membrane (6) and peroxisome (4), and homo-oligomerization by several monomeric subunits has recently been demonstrated in ABCG2 (42). Among mitochondrial ABC transporters, Mdl1 and M-ABC1 have been shown to oligomerize, but their partners remain unidentified (30, 43). We sought to elucidate the assembly partners, if any, of ABCB10 using a chemical cross-linking methodology. DFDNB, an amino-reactive noncleavable cross-linker with a short spacer arm (<3 Å), has been employed previously for protein structure studies (44). We used it here to identify assembly partners of ABCB10 that are not preserved using conventional SDS-PAGE techniques. Co-transfection and immunoprecipitation experiments of cross-linked mitochondrial preparations found that the dimerization partner for ABCB10 is an additional ABCB10 monomer. Mass spectrometry analysis of immunopurified ABCB10 complexes verified that ABCB10 homodimerizes and homo-oligomerizes in mitochondria and indicated that other proteins do not intimately co-assemble with ABCB10. Nonreducing SDS-PAGE suggests that the homodimer is stabilized through disulfide bonds, indicating that the dimeric association is sufficiently close to allow covalent bonding. Whether these bonds are natural or

artificial is unknown, for it was recently reported that oxidation during sample preparation may cause disulfide bond formation between dimeric units (42). Since no additional proteins intimately co-assemble with ABCB10, homo-oligomers of ABCB10 may themselves achieve functionality. Interestingly, homo-oligomerization of Δ105-ABCB10 appears to occur in the ER equally as efficiently as wild-type, mitochondria-localized ABCB10, suggesting that the process does not require the mTP of ABCB10 or any mitochondria-specific chaperones.

Acknowledgments—We thank Jim Pearson and Eric Cecil for important contributions; Stuart Orkin for valuable advice; Louis Kerr for technical support with confocal microscopy; Roland Lill for helpful discussions; and Dani Dagan, Eva Czerwiec, Mark Messerli, Jakob Wikstrom, Thorsten Schlaeger, and Shana Katzman for critical review of the manuscript.

REFERENCES

1. Higgins, C. F. (1992) *Annu. Rev. Cell Biol.* **8,** 67–113
2. Holland, B., Cole, S. P. C., Kuchler, K., and Higgins, C. F. (2003) *ABC Proteins: From Bacteria To Man*, Academic Press, Inc., San Diego
3. Schmitt, L., and Tampe, R. (2002) *Curr. Opin. Struct. Biol.* **12,** 754–760
4. Liu, L. X., Janvier, K., Berteaux-Lecellier, V., Cartier, N., Benarous, R., and Aubourg, P. (1999) *J. Biol. Chem.* **274,** 32738–32743
5. van Veen, H. W., Margolles, A., Muller, M., Higgins, C. F., and Konings, W. N. (2000) *EMBO J.* **19,** 2503–2514
6. Kage, K., Tsukahara, S., Sugiyama, T., Asada, S., Ishikawa, E., Tsuruo, T., and Sugimoto, Y. (2002) *Int. J. Cancer* **97,** 626–630
7. Lill, R., and Kispal, G. (2001) *Res. Microbiol.* **152,** 331–340
8. Shirihai, O. S., Gregory, T., Yu, C., Orkin, S. H., and Weiss, M. J. (2000) *EMBO J.* **19,** 2492–2502
9. Mitsuhashi, N., Miki, T., Senbongi, H., Yokoi, N., Yano, H., Miyazaki, M., Nakajima, N., Iwanaga, T., Yokoyama, Y., Shibata, T., and Seino, S. (2000) *J. Biol. Chem.* **275,** 17536–17540
10. Taketani, S., Kakimoto, K., Ueta, H., Masaki, R., and Furukawa, T. (2003) *Blood* **101,** 3274–3280
11. Shimada, Y., Okuno, S., Kawai, A., Shinomiya, H., Saito, A., Suzuki, M., Omori, Y., Nishino, N., Kanemoto, N., Fujiwara, T., Horie, M., and Takahashi, E. (1998) *J. Hum. Genet.* **43,** 115–122
12. Csere, P., Lill, R., and Kispal, G. (1998) *FEBS Lett.* **441,** 266–270
13. Chacinska, A., Pfanner, N., and Meisinger, C. (2002) *Trends Cell Biol.* **12,** 299–303
14. Horwich, A. L., Kalousek, F., and Rosenberg, L. E. (1985) *Proc. Natl. Acad. Sci. U. S. A.* **82,** 4930–4933
15. Schatz, G., and Dobberstein, B. (1996) *Science* **271,** 1519–1526
16. Schwarz, E., and Neupert, W. (1994) *Biochim. Biophys. Acta* **1187,** 270–274
17. von Heijne, G. (1986) *EMBO J.* **5,** 1335–1342
18. Duby, G., Oufattole, M., and Boutry, M. (2001) *Plant J.* **27,** 539–549
19. Obita, T., Muto, T., Endo, T., and Kohda, D. (2003) *J. Mol. Biol.* **328,** 495–504
20. Gakh, O., Cavadini, P., and Isaya, G. (2002) *Biochim. Biophys. Acta* **1592,** 63–77
21. Voos, W., Martin, H., Krimmer, T., and Pfanner, N. (1999) *Biochim. Biophys. Acta* **1422,** 235–254
22. Kurz, M., Martin, H., Rassow, J., Pfanner, N., and Ryan, M. T. (1999) *Mol. Biol. Cell* **10,** 2461–2474
23. Wiedemann, N., Pfanner, N., and Ryan, M. T. (2001) *EMBO J.* **20,** 951–960
24. Gregory, T., Yu, C., Ma, A., Orkin, S. H., Blobel, G. A., and Weiss, M. J. (1999) *Blood* **94,** 87–96
25. Hjelmeland, L. M. (1990) *Methods Enzymol.* **182,** 253–264
26. Wilcox, S. K., Cavey, G. S., and Pearson, J. D. (2001) *Antimicrob. Agents Chemother.* **45,** 3046–3055
27. Glick, B. S. (1991) *Methods Cell Biol.* **34,** 389–399
28. Emanuelsson, O., von Heijne, G., and Schneider, G. (2001) *Methods Cell Biol.* **65,** 175–187
29. Ma, Y., and Taylor, S. (2002) *J. Biol. Chem.* **277,** 27328–27336
30. Hogue, D. L., Liu, L., and Ling, V. (1999) *J. Mol. Biol.* **285,** 379–389
31. Zhang, F., Hogue, D. L., Liu, L., Fisher, C. L., Hui, D., Childs, S., and Ling, V. (2000) *FEBS Lett.* **478,** 89–94
32. Abe, Y., Shodai, T., Muto, T., Mihara, K., Torii, H., Nishikawa, S., Endo, T., and Kohda, D. (2000) *Cell* **100,** 551–560
33. Schatz, G. (1997) *Nature* **388,** 121–122
34. Arnold, I., Folsch, H., Neupert, W., and Stuart, R. A. (1998) *J. Biol. Chem.* **273,** 1469–1476
35. Galanis, M., Devenish, R. J., and Nagley, P. (1991) *FEBS Lett.* **282,** 425–430
36. Stan, T., Brix, J., Schneider-Mergener, J., Pfanner, N., Neupert, W., and Rapaport, D. (2003) *Mol. Cell. Biol.* **23,** 2239–2250
37. Glaser, S. M., Miller, B. R., and Cumsky, M. G. (1990) *Mol. Cell. Biol.* **10,** 1873–1881
38. Robin, M. A., Anandatheerthavarada, H. K., Biswas, G., Sepuri, N. B., Gordon, D. M., Pain, D., and Avadhani, N. G. (2002) *J. Biol. Chem.* **277,** 40583–40593
39. Addya, S., Anandatheerthavarada, H. K., Biswas, G., Bhagwat, S. V., Mullick, J., and Avadhani, N. G. (1997) *J. Cell Biol.* **139,** 589–599
40. van Leeuwen, H. C., and O'Hare, P. (2001) *J. Cell Sci.* **114,** 2115–2123
41. Ramjeesingh, M., Ugwu, F., Li, C., Dhani, S., Huan, L. J., Wang, Y., and Bear, C. E. (2003) *Biochem. J.* **375,** 633–641
42. Xu, J., Liu, Y., Yang, Y., Bates, S., and Zhang, J. T. (2004) *J. Biol. Chem.* **279,** 19781–19789
43. Young, L., Leonhard, K., Tatsuta, T., Trowsdale, J., and Langer, T. (2001) *Science* **291,** 2135–2138
44. Krupenko, S. A., Kolesnik, O. I., Krupenko, N. I., and Strel'chyonok, O. A. (1995) *Biochim. Biophys. Acta* **1235,** 387–394